Soils and Rocks
www.soilsandrocks.com
An International Journal of Geotechnical and Geoenvironmental Engineering
ISSN 1980-9743
ISSN-e 2675-5475

Seismic zoning of Tabriz area by stochastic finite fault model considering site-specific soil effects

Armin Sahebkaram Alamdari[1], Rouzbeh Dabiri[1#], Rasoul Jani[1], Fariba Behrouz Sarand[1]

Article

Keywords
Tabriz
Tabriz North Fault
Seismic zonation
Peak ground acceleration
Stochastic finite fault

Abstract

Tabriz, as one of the most earthquake-prone cities in the Iran plateau, has experienced enormous earthquakes that have even destroyed the city altogether. Considering this seismological background and the vicinity of Tabriz's northwestern fault, reducing the possible earthquake losses can be highly useful by scrutinizing the strong ground motion resulting from the fault activation. To this end, a stochastic finite-fault ground motion simulation (EXSIM) method was applied as an important means for predicting the ground motion near the epicenter of the earthquake. EXSIM is an open-source stochastic finite-fault simulation algorithm that generates the time-series of the earthquake's ground motion. Based on the findings, the peak horizontal acceleration reached 0.83 g in the northern parts by creating artificial accelerograms and Tabriz's seismic zonation. In comparison, it reduced by 0.48 g by departing from the fault in the city's southern parts. Additionally, providing a seismic zonation map in Tabriz revealed that stopping the construction in the north parts while extending the settlement construction to the south part of the city are considered vital and unavoidable. Also, by applying the magnification and effects of the soil layers above the bedrock, it was further found that the existence of the loose layer with low strength and compaction intensify the application of seismic acceleration on the near-surface structures in the central, west, and southwest parts of the target area.

1. Introduction

The earthquake is regarded as one of the natural hazards that puts an end to many people's lives. Various studies have globally delved into finding appropriate methods to counteract and reduce the caused damage by predicting the amount of the released energy by fault activation. The Iranian plateau is formed by the active tectonics of the Alpine-Himalayan seismic belt and is located between the tectonic plates of Eurasia and Arabia. This plateau is also considered one of the most seismic-prone regions in the world that face many earthquakes per year (Mirzaei, 1997). Several parameters contribute to the need for special attention to this natural risk, including the active tectonic conditions, the presence of faults, and numerous seismogenic sources, along with the high population density in areas susceptible to the earthquake (Zaré et al., 1999; Uyanık, 2015). Given the above-mentioned seismic conditions regarding the Iran plateau, many studies have extensively focused on this area (e.g., Nowroozi, 1996; Shoja-Taheri, 1984; Nogol-Sadat, 1994; Jackson at al., 1995; Tavakoli, 1996; Mirzaei et al., 1998; Berberian & Yeats, 1999; Zaré & Memarian, 2000; Masson et al., 2006; Ansari et al., 2009; Karimiparidari et al., 2011; Hamzehloo et al., 2012; Mojarab et al., 2013; Khoshnevis et al., 2017).

Besides, numerous cities have been expanded in the range of active faults despite this vast area's seismicity. Among these metropolises, Tabriz is located in a seismicity area and has frequently been faced with earthquakes throughout its history. According to Berberian (1976), Tabriz's most dramatic earthquake occurred in the 1780 with a magnitude of 7.7, leading to the city's destruction. This city is surrounded by the mountains and plains of Tabriz from the North, South, and East, the Talkhehrood salt marshland (Ajichai) from the West, and is shaped like a fairly large hole or a hinterland plain. Besides, the North Tabriz Fault is the most dangerous in Iran due to extensive construction volume and population density. Moreover, this fault is even more dangerous than the North Tehran Fault, Alborz and Zagros, and other Iran faults. The city of Tabriz shakes if the earthquake occurs, but the landslide and rupture occur in the north and east of the metropolis, located on the fault.

Similarly, the North Tabriz Fault with the right-lateral strike-slip mechanism of pressure component (such that in most parts, northern limb raises more compared to the southern limb) is considered a seismic and active fault with at least 16 historical earthquake occurrences (Zaré, 2000). Moreover, as one of the most prominent faults in Azerbaijan, this fault

#Corresponding author. E-mail address: rouzbeh_dabiri@iaut.ac.ir
[1]Department of Civil Engineering, Tabriz Branch, Islamic Azad University, Tabriz, Iran.

Submitted on January 20, 2020; Final Acceptance on November 20, 2020; Discussion open until May 31, 2021.

DOI: https://doi.org/10.28927/SR.2021.047220

is extended along the main road of Tabriz-Boustanabad up to Miyaneh and has caused an earthquake with a magnitude of 7.6 Richter scale in 1721 (Berberian, 1976; Berberian & Yeats, 1999). Although the fault has no definite activity in the current century, there is some evidence on its possible remotion. Statistical data also show that the return period of severe and destructive earthquakes in Tabriz can reach about 260 years. We can refer to some studies that have addressed the above issue (e.g., Zaré, 2001; Zaré et al., 2009; Manafi, 2012; Farahani, 2015). The geometry of the fault was determined based on geological information, seismology, and existent equations (Ambraseys & Melville, 1982; Wells & Coppersmith, 1994; Siahkali Moradi et al., 2008). It has been mentioned in Table 1.

The study area of Tabriz is selected in this work because the earthquake system record does not record any destructive event for Tabriz fault, and the estimation of strong ground motion predicts based on the hypothetical stochastic model in this region. Simulating the earthquakes scenario is the best method for getting more knowledge of the Tabriz region's earthquake event.

Accordingly, in the research regarding the significance of the seismicity of Tabriz and its location in the vicinity of the Tabriz fault, the peak horizontal acceleration was calculated, and the seismic zonation map of the study area due to the activation of Tabriz fault provided using the stochastic finite-fault method by selecting appropriate parameters. Then, the peak horizontal acceleration near the surface was computed utilizing the seismic zonation results of Tabriz urban area and collecting geotechnical and geophysical down hole sampling from different points of the target area by applying the soil's magnification effects layer.

2. Literature review

2.1 Stochastic finite fault

Given the issues mentioned above and the importance of the subject in this research, Tabriz's seismic zonation considering due to the activation of the North Tabriz Fault. For this purpose, the stochastic finite fault method is employing to predict the strong ground motion.

The stochastic finite-fault model is an important instrument for predicting the earth's motion near the epicenter of the earthquake. In strong ground motion modeling, the earthquake can be regarded as a point source when the target area is far from the earthquake source (fault). However, cases such as fault geometry, heterogeneous slip distribution on the fault surface, and directivity can greatly impact motion content in the near field (Boore, 2005, 2009). To investigate the effects of these finite faults on the ground motion modeling Hartzell (1978) suggested that an earthquake's fault surface is divided into a network of sub-faults, each of which can be considered a point source. Moreover, a fault surface is categorized into an array of sub-faults based on the determined magnitude according to its seismic moment, each one of which is treated as a point source.

Table 1. The Geometry of North Fault of Tabriz.

Section	Value
Length and width of the fault (km)	19.9×150
Strike slope	85 310

Additionally, the sub-faults' time-series employs a serialized point-source stochastic model, developed by Boore (1983, 2003), using the stochastic method simulated by generalized computer code (Boore, 2003, 2005). Various studies have sought to obtain the maximum strong ground motion utilizing a stochastic finite fault in recent years. For instance, Scandella et al. (2011) investigated the earthquake scenario in Vicoforte, Italy, applying the kinematic source developed by Hisada & Bielak (2003) and the stochastic finite fault. Similarly, Zonno et al. (2012) presented the high-frequency maximum observable shaking map of Italy for the fault source. Besides, Yazdani & Kowsari (2013) provided the earthquake ground-motion prediction equation for northern Iran using the same method. Using the stochastic finite fault method, Samaei et al. (2014) also conducted a study on the strong ground motion from Niavaran fault in Tehran. Likewise, Wang et al. (2015) simulated the 2013 Lushan earthquake in China with a 7 Richter scale by the field acceleration approach.

Moreover, Amiranlou et al. (2016) predicted the strong ground motion of Tabriz's north fault utilizing the stochastic finite fault model based on a dynamic corner frequency simulation. Eventually, Karimzadeh et al. (2019) simulated a vast range of ground motion, followed by simulating a large collection of simulated earth movements. They then studied the effects of various parameters on the seismic behavior of a single degree of freedom systems in terms of energy, applying a nonlinear time history analysis. Finally, stochastic finite fault simulations were conducted on the western parts of the Northern Anatolian Fault zone in Turkey.

2.2 Seismic amplification

Destructions resulted from the recent earthquakes reveal the effect of site conditions and topography on the severity and extent of destructions. Therefore, investigating these factors on the seismic wave response is of great importance in earthquake engineering. Complex topographic feature patterns cause significant differences in arriving the waves to the ground surface. Furthermore, surface and sub-fault ruggedness increase the range of ground motion. The influence of local soil conditions on ground motion characteristics has long been revealed while the earthquake waves travel through the soil layers and arrive at the ground surface. Previous studies demonstrated soil layer characteristics, including the type, depth, and profile of the soil effect on the ground response domain, even in moderate earthquakes, and highlighted them as important factors for ground motion estimation (Yaghmaei-Sabegh & Motallebzade, 2012).

For example, Rodríguez-Marek et al. (2001) introduced a simple empirical approach based on the seismic site response, including the dynamic stiffness of surficial material measurement and the bedrock's depth. This geotechnical site classification scheme provides an alternative to the geologic-based and shear wave. Similarly, Pitilakis et al. (2004) conducted a study on the environmental regulation setting's design response spectra and soil classification. Moreover, Park & Hashash (2005) evaluated seismic site factors in the Mississippi Embayment and analyzed the probabilistic seismic hazard with nonlinear site effects. Hashash et al. (2010), besides reviewed recent advances in nonlinear site response analysis focusing on 1-D site response commonly used in engineering practice. He described material models' developments for both total and effective stress considerations and the challenges of capturing the measured small and large strain damping within these models. Additionally, Eker et al. (2012) investigated local site characteristics, and seismic classification study using active and inactive wave approaches in the north of Ankara, Turkey. Likewise, in their study, Drennov et al. (2013) examined the acceleration response spectra of earthquakes with M=4-6.5 in the southwestern part of the Baikal Rift Zone. Also, Uyanık et al. (2013) determined from shear wave velocity the soil liquefaction locations of soils in Kumluca district with assuming an earthquake to be M=7 in the Finike–Kaş–Elmalı triangle in the southwest of Antalya, Turkey. Also, Groholski et al. (2014) conducted a study regarding the dynamic soil behavior and pore pressure response from Downhole array measurements. More, Atesh & Uyanık (2019) applied the spectral ratio and horizontal to vertical spectral ratio techniques to earthquake signals using the reference and single station methods to determine the amplification of the building and ground in Kocaeli, Turkey. Verdugo et al. (2019) also presented an alternative method to establish seismic site classification. It is noteworthy that the use of the new spectral parameters named "Spectral Threshold Displacement (STD)" and "Spectral Threshold Acceleration (STA)" allow identifying the relevance of the displacement spectrum with the structural damage, which is also related to the stiffness and drift of the structure. Besides, Shreyasvi et al. (2019) attempted to combine the local site response with the standard probabilistic seismic hazard analysis. The site response was computed by performing an equivalent linear analysis in the frequency domain. Yaghmaei-Sabegh & Hassani (2020) developed a new site amplification model for Iran based on the site fundamental frequency obtained from the horizontal-to-vertical spectral ratio.

3. Method

3.1 Stochastic finite-fault modeling

Possible simulation methods are of two types: in the first type, the seismic source is a point source; in the second type, which is called finite fault simulation, the seismic source is a rectangular fault that in its longitudinal and transverse directions as sources the point is of the same elements. The point source method cannot consider the main parameters of an earthquake in a massive earthquake, such as the long duration and the slopes' dependence on the observation station (orientation effect). Due to these limitations, the modeling method based on finite faults proposed by Hartzel and has become very popular in the last two decades (Boore, 2009).

The finite fault modeling method combines the plane source aspects with the point source seismic model, and since the mentioned limitations do not naturally exist in the limited fault modeling method, this geometry method fails and considers the effect of orientation and gives good results. For simulation using finite faults, the time delay method, and addition of related accelerometers of a two-dimensional network containing elements, are used. The stochastic point source method is using in cases where the distance of the fault from the study area is so far that the fault can study as a point relative to the case study, but in cases where the distance from the fault is very close or the part of the study area located on the fault, it is better to use the stochastic finite fault method (Boore, 2009).

Motazedian & Atkinson (2005) proposed simulating earthquake seismogram using the stochastic finite-fault method relying on dynamic corner frequency. Based on their findings, high accurate results were obtained by improving the approach and increasing more parameters. In this model, the corner frequency was a function of time, and the rupture history controlled the frequency content of the simulated time series of each sub-fault. A large fault was also divided into N sub-faults, where each sub-fault was considered a small point source (Figure 1).

EXSIM is an open-source stochastic finite-fault simulation algorithm, which is written in FORTRAN that generates the time series of the ground motion for the earthquakes (Atkinson & Assatourians, 2015). In the finite fault modeling of the ground motion, a large fault is categorized into N sub-faults, where each sub-fault is considered a small point-source. The ground motion that contributed to each sub-fault can be calculated by the stochastic point-source method and then summed at the observation point with a proper time delay to obtain the ground motion from the entire fault.

The time series from the sub-faults are modeled using the point-source stochastic model developed by Boore (1983, 2003) and popularized by the Stochastic-Method Simulation computer code (Boore, 2003, 2005). Furthermore, each sub-fault's ground motion is treated as the random Gaussian noise of a specified duration by having an underlying spectrum as given by the point-source model (Brune, 1970) for shear radiation. This basic idea was implemented in many studies (e.g., Irikura 1983, 1992; Schneider et al., 1993; Irikura & Kamae, 1994; Atkinson & Silva, 1997; Bour & Cara, 1997; Beresnev & Atkinson, 1998; Motazedian & Atkinson, 2005; Boore, 2009). Motazedian & Atkinson (2005) introduced the new variety of this method based on dynamic corner frequency. Their implementation had a significant advantage

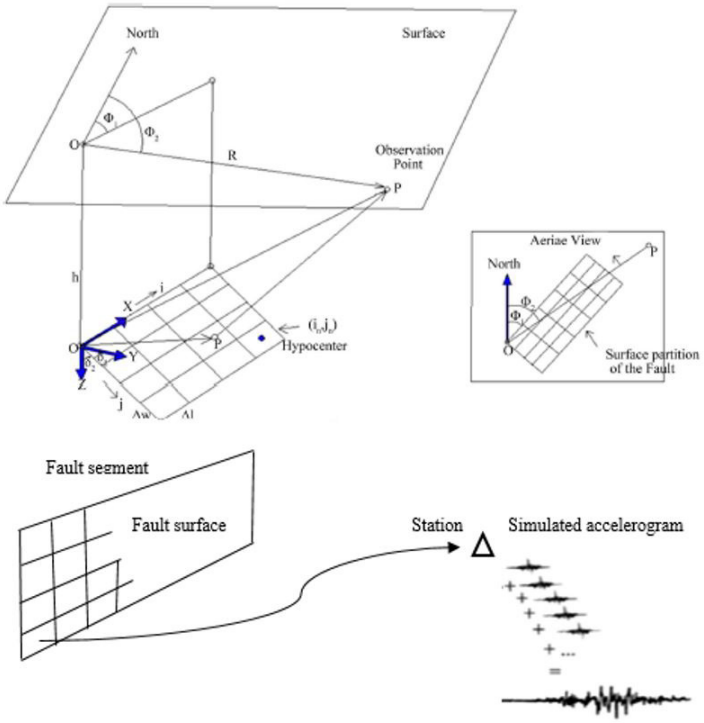

Figure 1. An illustration of finite-fault modeling. The fault surface divides into smaller fault segments, and each subfault is treating as a point source (Motazedian & Atkinson, 2005).

over previous algorithms such that it made the simulation results relatively insensitive to the sub-fault size and thus eliminated the need for the multiple triggering of the sub-events (Atkinson & Assatourians, 2015). Boore (2009) moreover improved the algorithm with modifications to the sub-event normalization procedures that eliminated the remaining dependency on sub-fault size and improved the treatment of low-frequency amplitudes. In this model, the corner frequency is a function of time, and the rupture history controls the frequency content of the simulated time series of each sub-fault.

Moreover, the rupture begins with a high corner frequency and progresses to lower corner frequencies as the ruptured area grows. Additionally, limiting the number of active sub-faults in calculating dynamic corner frequency can control the amplitude of lower frequencies. In the revised EXSIM algorithm, properly normalized and delayed sub-fault contributions are summed in the time domain as

$$A(t) = \sum_{i=1}^{N} H_i \times Y_i\left(t - \Delta t_i - T_i\right) \quad (1)$$

$$H_i = \frac{M_0}{M_{0_i}} \sqrt{\frac{\sum_j \left(\frac{f_0^2 f_i}{f_0^2 + f_j^2}\right)^2}{N \sum_j \left(\frac{f_{0_i}^2 f_i}{f_{0_i}^2 + f_j^2}\right)^2}} \quad (2)$$

A(t) is the total seismic signal at the site, which incorporates the sub-faults' delays. Besides, H_i denotes a normalization factor for *i*th sub-fault that aims to conserve high-frequency amplitudes. Further, Y_i (t), N, and Δt_i indicate the signal of the *i*th sub-fault (the inverse Fourier transform of the sub-fault spectrum), the total number of sub-faults, and the delay time of the sub-fault, respectively. Furthermore, T_i and M_0 are a fraction of the rise time and the total seismic moment. Finally, M_{0i} displays the seismic moment of *i*th sub-fault, which is internally calculated by the EXSIM based on the sub-fault size (Atkinson & Assatourians, 2015; Atkinson et al., 2011). The final version of EXSIM named "EXSIM12" by Atkinson & Assatourians (2015) was used in the present research.

3.2 Site response analysis

Various evidence were reported regarding the site effect and nonlinear behavior of the local soil in previous earthquakes. The soil type and thus the dynamic characteristics of the soil profile (e.g., attenuation and shear modulus, soil liquefaction, soil amplification, porosity, moisture content, the number of layers, and their thickness) were all mentioned as factors that affect the nonlinear behavior of the soil (Uyanık et al., 2006; Eker et al., 2012; Drennov et al., 2013).

Many researchers investigated the effects of different parameters on seismic magnification. For example, Park & Hashash (2005) and Rodríguez-Marek et al. (2001) highlighted soil thickness as one of the most significant parameters for the seismic response. Pitilakis et al. (2004) and Uyanık (2015) also considered the very high effect of

different variables on seismic bedrock, including the soil type, soil classification and thickness, the dominant period of the local soil, and the average velocity of shear wave in the alluvial layer.

It is noteworthy that in the current study, the DEEPSOIL software, which is applied for site response analysis, was used for seismic magnification. DEEPSOIL is a unified one-dimensional program utilized for the dynamic analysis of the site response in linear, equivalent-linear, and nonlinear approaches. Moreover, this software provides the user with the required outputs by accelerograms and the applying site conditions (Hashash et al., 2016). The linear approach was utilized in this research, as well.

In this method, a conversion function with dynamic and force properties was determined based on one of the bedrock's dynamic properties. This approach, based on the principle of force summation, is a very simple method and is based on complex number calculation. The bedrock motion, which is considered accelerograms, can be converted to the Fourier series that can be changed into the Fourier series of the used conversion function's ground motion. Thus, the conversion function easily determines the resonance or damping of the bedrock motion when it arrives at the surface.

In this study, we first investigate the input parameters for the stochastic finite fault model by investigating the North Tabriz Fault and the Tabriz city area survey. Then, due to the importance of correctly selecting input parameters using empirical reduction relationships, the selected input parameters have been validated. By obtaining modeling results using stochastic finite fault, maximum acceleration seismic zonation due to activation of North Tabriz Fault over the studied area is presented.

Finally, by collecting geotechnical (to obtain general and soil strength characteristics) and geophysical (to obtain the shear wave velocity of the soil) data by Downhole sampling, from reputable and active laboratories in this field (Like the results of geotechnical and geophysical experiments that have been done in the study phase of different lines of Tabriz metro.), and experiments have performed in areas where there is not enough data seismic magnification is carrying out by transferring seismic acceleration from bedrock to ground level using Deepsoil software. The calculation of the results will show us the maximum seismic acceleration at ground level. The aggregation of results provides a zoning map for maximum seismic acceleration at ground level for the Tabriz city area. Figure 2 schematically illustrates the present study.

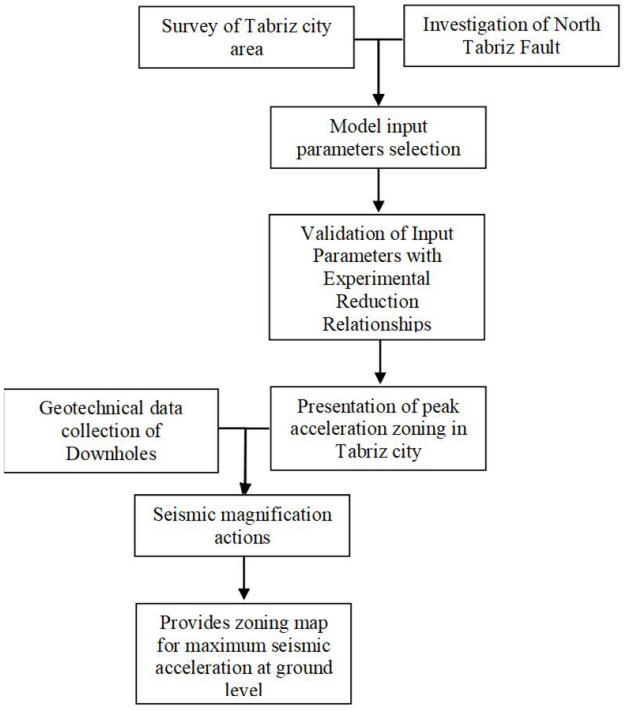

Figure 2. Schematic of progressive research.

4. Case study

4.1 Tabriz boundary

Tabriz city is located in the northwest of Iran, near one of the most important and known seismic faults of the Iranian Plateau (North Tabriz Fault). The North Tabriz Fault with its right-lateral strike-slip mechanism of pressure component (such that in most parts, the northern limb has raised more than the southern limb) is regarded as a seismic and active fault with at least 16 historical earthquakes occurring. Additionally, it is a well-known fault of Iran's seismic faults due to the historical earthquake occurring and the destruction of Tabriz for 12 times. The fault is currently laying on through the settlements in the north of Tabriz, owing to the expansion of construction and settlement construction on the fault zone. The losses and massive damages for an earthquake of a magnitude of 6.5 or more are predicted based on the risk of the direct rupture in the city, the faulting within Tabriz boundary, and the effects of the near-field fault. Besides, the evaluation of seismic potential and seismic zoning is of great importance due to Tabriz's significance in the northwestern parts of Iran, the history of seismicity, the existence of marl-clay deposits, and the potential for landslides (Zaré, 2001).

4.2 Geotechnical conditions of the study area

Based on the studies done on alluvial sediments and the data obtained from drilled wells in Tabriz, the thickness of alluvial sediments in different parts of the city is different. The thickness of these sediments increases from east to west. Most of which are the clay, silt, and sand. The thickness of the alluvium decreases from the city center to the north and south of the city. North and northeast towns of Tabriz (Eram and Baghmisheh) on Miocene units and several neighbourhoods and towns east, south, northeast of Tabriz (Valiasr town, El Goli, Sahand's Villashahr and Andisheh) on lignite layers and Miocene and Miocene-

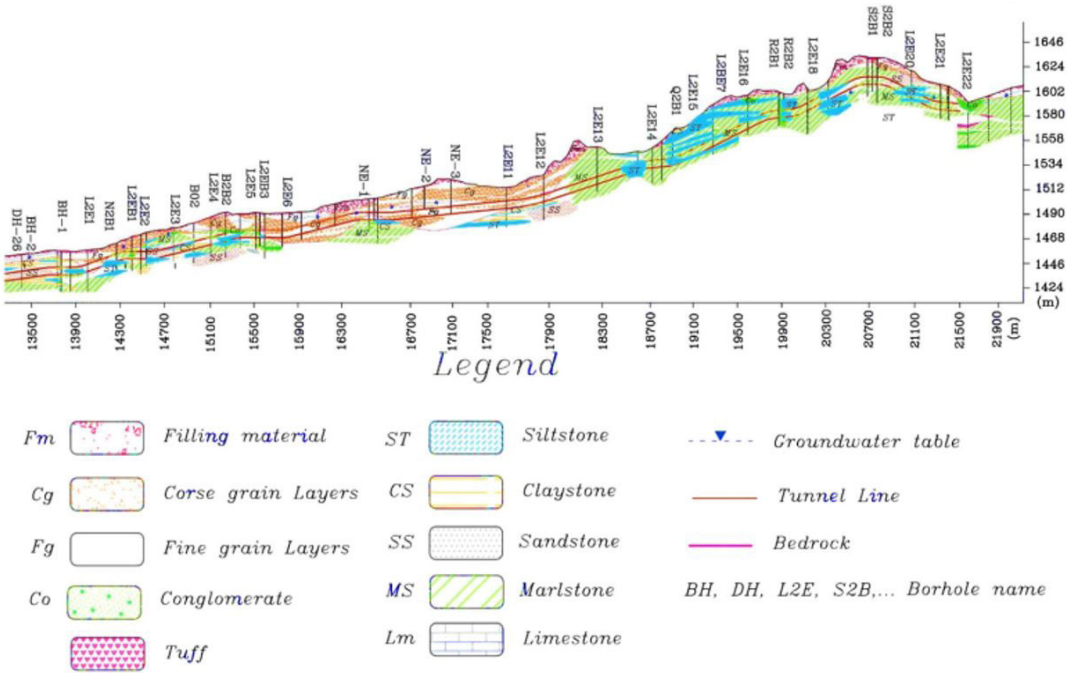

Figure 3. Geotechnical section of the western part of tunnel route line 2 of Tabriz's metro (Mohammadi et al., 2016).

Pliocene age fish and Sahand pyroclastic units of Pliocene to Early Quaternary age. The central part of the city is also located on alluvial sediments.

Based on the geological and groundwater data obtained from boreholes of the western part of tunnel route line 2 of Tabriz's metro, Figure 3 shows the boreholes and soil layers' location. Geologically, this part of the tunnel comprises sedimentary rocks consisting of marls, claystone, siltstone, and sandstone, which are underlain by surface alluvium with a thickness of 5-15 m. In this part, the water table varies between 6 and 30 m, and the consistency of the alluvium is classified as hard and very hard (Mohammadi et al. 2016).

As the former Yaghmaei-Sabegh & Hassani (2020) have pointed out, the most intensification occurs in soft soil layers, which Vs30 is usually less than 175. Therefore, it is expected that in areas with denser alluvial layers, the maximum intensification of peak ground acceleration will be observed.

4.3 The North Tabriz Fault

As mentioned earlier, the North Tabriz Fault was the target fault in this study. The daily mild motion and shaking of the ground occur in Tabriz. The placement of Alborz and Zagros Mountain ranges and Tabriz, located at the intersection of these two mountains, in the Alpine belt, is the reason for the large and destructive earthquakes in these areas. The belt originates from the middle of the Atlantic and crossing the Mediterranean Sea, north of Turkey, Iran, India, China, and the Philippine Islands and merges to another belt that revolves around the Pacific Ocean. Evidence shows that this fault is about 150 km long and its rupture can be very hazardous due to its location within the Tabriz metropolitan area. As referred before, the North Tabriz Fault is the longest active one with a significant portion within the urban area. According to the constructions done on North Tabriz Fault, this fault is called the most dangerous fault of the Iranian plateau. Other faults in the Iranian plateau either have a far distance that reduces their impact on the study area or do not have the power to create maximum acceleration and magnitude as the North Tabriz fault. Therefore, the North Tabriz Fault is considered as the main fault.

The length, wide, and the dip of the fault are 150 km, 12 km, 87 degrees, respectively, and its seismicity depth is estimated about 10 to 20 km based on the recorded micro-seismic data which are classified as surface earthquakes (Ambraseys & Melville, 1982; Wells & Coppersmith, 1994).

4.4 Input parameters

Table 2 presents the key input parameters for simulating the artificial seismogram for Tabriz's north fault by the stochastic finite-fault method using the EXSIM program.

4.5 Validation of input parameters

To validate and control the opted parameters' correction, a comparison was made between an initial modeling and the scaling relationships that indicated the maximum ground-motion parameters as a function of magnitude and distance. For this purpose, it was included four scaling relationships were developed by Sinaiean et al. (2007), Boore & Atkinson (2008), Campbell & Bozorgnia (2008), and Boore et al.

Table 2. The Input Parameters for Simulation.

Input Parameters of EXSIM	Value
Fault orientation (strike)	310°
Fault orientation (dip)	87°
Fault depth to upper edge (km)	5
Sub-fault dimensions (km)	2×2
Moment magnitude	7.5
Stress drop (bar)	60
Geometric spreading	$\frac{1}{R}$, $R \leq 85$ km $\frac{1}{R^{0.5}}$, $85<R<120$ km $\frac{1}{R^{0.5}}$, $R \geq 120$ km
Quality (Q) factor (f)	$95 f^{0.8}$
Distance-dependent duration	$T_0 + 0.1R$
Kappa coefficient	0.03
Pulsing area	50%
Windowing function	Saragoni-Hart
Shear-wave velocity (km/s)	3.3
Rupture velocity	$0.8 \times$ Shear wave velocity
Density (gr/cm^3)	2.8
Damping	5%
Starting rupture element	Random
Slip distribution	Random

The values of the software input parameters were extracted from previous studies (e.g., Wells & Coppersmith, 1994; Kanamori & Anderson, 1975; Anderson & Hough, 1984; Farahbod & Alahyarkhani, 2003; Hoseinpour & Zaré, 2009; Motazedian, 2006; Sinaiean, 2006).

(2014). Good agreement with Iran's earthquakes was the reason for their selection (Shoja-Taheri et al., 2010). Figure 4 displays a comparison among the obtained results of these four relationships with the initial ESXIM12 model.

The data depict the peak accelerating values of the initial modeling, along with the mentioned scaling relationships. As shown, there is a good agreement among the results of the initial model and scaling relationships, which shows that the selected input parameters for modeling the North Tabriz Fault have been selected correctly. As pointed in the presented results, the prediction equation presented by Sinaiean et al. (2007) predicts a maximum acceleration greater than the other equations near the fault, and the other results of the prediction equations are in complete agreement. However, the equation of Campbell & Bozorgnia (2008) with distance from the fault predicted a smaller maximum acceleration prediction.

The similarity of most of the predicted equations is in the input parameters, magnitude (M), fault length (R), soil shear wave velocity (V_{s30}), and distance from the fault (Z), which are used in all relations for validation. The original model was the same. This shows the importance and high impact of these parameters in the output of the presented results, which should be paid special attention to the correct selection of these parameters. However, some researchers, such as Boore et al. (2014), consider other parameters in the proposed method, such as the focal mechanism and the type of fault.

5. Modeling of the North Tabriz Fault

5.1 Zonation of peak acceleration in Tabriz boundary

After selecting the appropriate modeling parameters, the simulation was conducted based on the mentioned parameters on the seismic bedrock surface. Figure 5 depicts the points of the simulation of strong ground motion. The Peak Ground Acceleration (PGA) is calculated from the answer summing to obtain the results of the accelerogram and plot them based on acceleration and distance. A sample of the produced accelerogram is displayed in Figure 6. As well as, Figure 7 shows a map of the chirp lines for the simulated maximum horizontal acceleration.

As depicted, the peak horizontal acceleration produced by Tabriz's northern fault reaches 0.83g in the northern part of the city. In contrast, the peak acceleration in the southern part decreases to 0.48g. The obtained prediction results are in

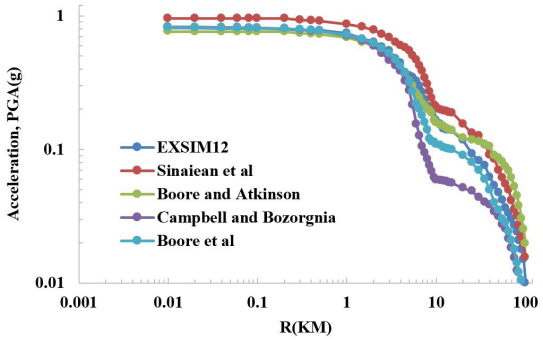

Figure 4. A comparison of PGA among the results of the empirical scaling relationship and initial EXSIM12 model.

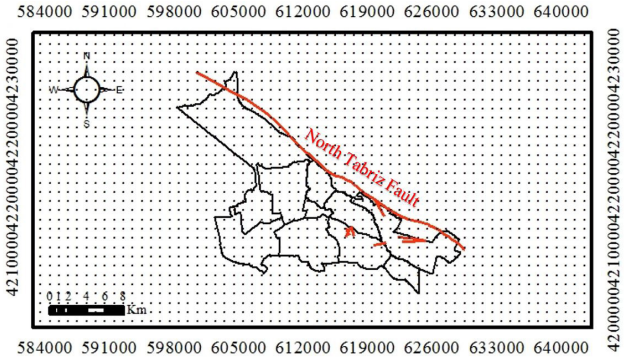

Figure 5. The points of artificially produced accelerograms.

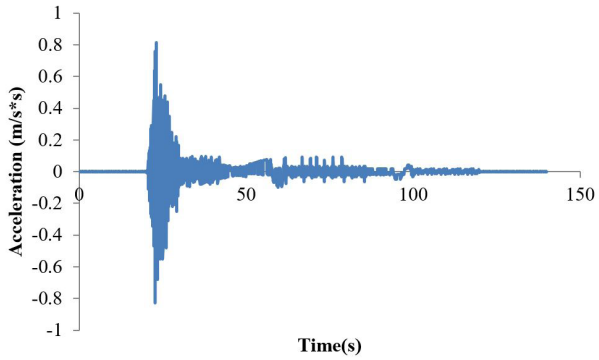

Figure 6. A sample of simulated accelerograms.

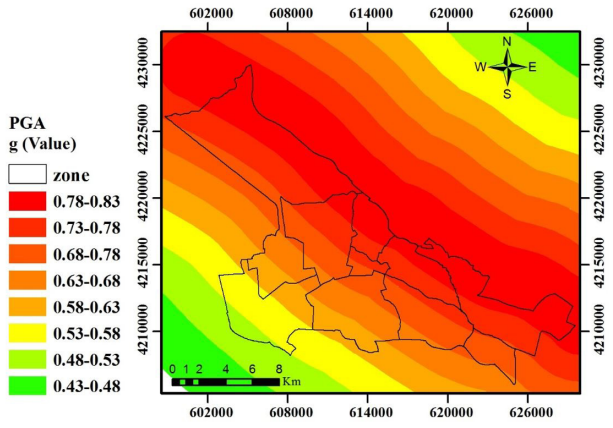

Figure 7. The chill lines map simulated for maximum horizontal acceleration.

good agreement with the results of Karimzadeh et al. (2014), who have obtained the peak ground acceleration due to the activation of the North Tabriz Fault by 0.3 to 0.8g using the Probabilistic Seismic Hazard Analysis (PSHA). Furthermore, the massive losses and destructions are estimated in Tabriz because of the direct rupture hazard in the city, the fault in the urban area on Tabriz, and the effects of a near-field fault the earthquake. In settlements such as Baghmisheh, Roshdieh, Eram, and Valiamr, at the northern part of Tabriz and near-field fault, there is a high potential for a landslide the marl-clay deposits. Given that Tabriz Airport is located in the near-field fault, earthquakes can cause serious destruction, leading to the disruption of assistance at the time of the possible earthquake.

In general, after an earthquake occurs inside the earth and the earth's energy is released, the energy released from its place of release, called the epicenter, propagates in the direction of vibration in all directions and carries the earthquake energy. These waves are very similar to the waves created by a rock falling into a pond's calm water. Just as a rock blow causes water waves to move, an earthquake creates seismic waves that propagate through the ground. The released energy is rapidly dispersed as it moves away from the epicenter, and due to the passage of rock and soil layers, it attenuates and decreases in intensity. That is the main reason for the maximum reduction of earthquake acceleration when moving away from the fault, known as the epicenter of an earthquake. The southern and southeastern parts of the area are more damped due to semi-dense conglomerate layers, but the southwestern and western parts of the area, due to the presence of young alluvial layers, maybe intensified in those areas, which are discussed in the next section.

5.2 Seismic peak acceleration at the surface

After obtaining the seismic zonation of the target area, 432 geotechnical and geophysical downhole data from different points of the urban area of Tabriz were gathered to assess the effect of soil stratification on the earthquake specification in terms of peak acceleration and frequency content. As shown in Figure 8, data from all points of the target area are used to have good distribution.

DEEPSOIL software was used to determine the peak ground acceleration at the surface and imply the amplification of the soil stratification effect. Accordingly, by having the seismic frequency in different points of the area, the gathered geotechnical characteristics (e.g., the soil layer thickness, specific gravity, the shear wave velocity of the soil layer, and attenuation in different layers) were utilized as the input variables for the software. Finally, the magnitude and effect of seismic frequency traveling from soil layers were determined in different samples. After collecting and presenting the results within the target area, seismic zonation after amplification on the ground surface using ArcMap software is depicted in Figure 9.

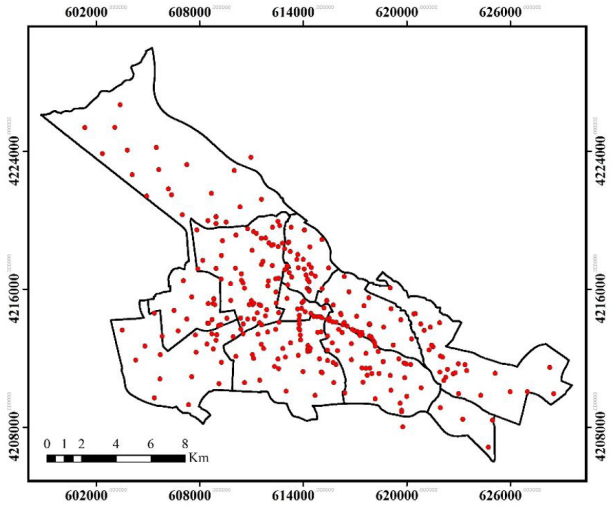

Figure 8. Distribution of collected data for seismic amplification.

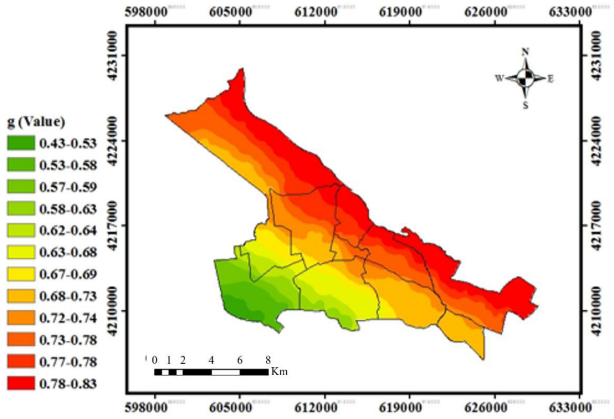

Figure 9. The seismic zonation of Tabriz surface after including soil layer and amplification factor.

The results show that in the north, east, and southeast of Tabriz, due to the low thickness of loose sedimentary deposits, the magnification of acceleration values is minimal. In contrast, the magnification of acceleration values in the western part of Tabriz has the highest rate due to the high thickness of sedimentary deposits. A comparison of acceleration maps calculated on the seismic bedrock and at the ground level shows the highest magnification areas, consistent with the magnification results performed by Amiranlou (2016).

Significant parameters in transmitting earthquake acceleration from bedrock to the ground surface are depth of subsurface, specific gravity, the hardness of subsoil, shear wave velocity in soil layers, soil layer damping, and shear wave hardness and velocity in bedrock. The most influential parameters are the shear wave velocities in the soil and bedrock layers, which change more the results are subject to further change.

6. Discussion

The current research evaluated Tabriz's urban area's seismic conditions and its location on the north of Tabriz's active fault. It was more attempted to determine the North Tabriz Fault's peak acceleration and provide the correct seismic zonation for the target area. For this purpose, the study applied a stochastic finite-fault method and EXSIM12 software. First, the initial model was verified, followed by examining this method's suitability for the target area by comparing its results with artificial accelerograms through the mentioned empirical relationships. The study then further evaluated the modeling parameters for the North Tabriz Fault that presented in Table 2. More efforts were made by comprehensively reviewing the references provided to select them correctly, which have a significant impact on the simulation results and showed how the modeling results could be sensitive to the input parameters like the effect of distance from the fault on the peak acceleration results and the influence of the presence of alluvial layers on the rate of peak intensification of seismic acceleration at the ground. Therefore, it is recommended to be extremely careful about selecting parameters and their compatibility with the selected model. Finally, by calculating the peak horizontal acceleration caused by the active North Tabriz Fault, it was observed that this value could increase up to 0.83 g in the northern part of Tabriz that occasionally lies on the fault. Still, in the southern part of the city, which is far from the fault, it decreased to 0.48 g. Considering the North of Tabriz's active fault, as well as the geotechnical conditions and landslide possibility and shaking at the due time of the earthquake, based on studies conducted by Karimzadeh et al. (2014) on the type and quality of structures and the effect of earthquakes on them, the buildings that have been constructed along the North Tabriz fault will be destroyed, and the buildings with a short distance will be very high destruction. Therefore, stopping the construction in the northern parts and continuing the settlement to the city's southern regions are inevitable.

In terms of assessing the resilience of vital uses of Tabriz city against earthquakes, the situation of the eastern, southeastern, and western regions of the study area is favorable. The western half of the northern and northwestern regions, especially the city center, which is the city's old texture and has high population density, have an unfavorable condition. Therefore, considering the improvement and renovation and observing the necessary regulations and standards, investment is recommended to make the existing vital uses more resilient and transfer and relocate essential services to other areas for Tabriz's central region (Mohammad Raza et al., 2018).

Based on the results related to the seismic zonation after implying the soil layer effects on the depth up to the bedrock and amplification, most of the site effect's consequences were observed in the central and center-west part of Tabriz city. A comparison of acceleration maps calculated on the seismic bedrock and at the ground level

shows the highest magnification areas, consistent with the magnification results performed by Amiranlou (2016). Such outcomes were due to the existence of the alluvial layers of the current age (i.e., west and southwest boundary) and the young alluviums (along the Goorichay River) and the presence of low resistant and density soil layers (Rustaei & Sari Sarraf, 2006). Eventually, these layers' effect on seismic acceleration intensity by amplification reached 15-20% in some points in the provided map.

7. Conclusion

The study further evaluated the modeling parameters for the North Tabriz Fault and showed how the results of the modeling could be sensitive to the input parameters. Therefore, it is recommended to be extremely careful about the selection of parameters and their compatibility with the selected model.

Peak ground surface acceleration caused by the active North Tabriz Fault was observed. This value could increase up to 0.83g in the northern part of Tabriz, which occasionally lies in the fault. Considering the active fault in the North of Tabriz, as well as the geotechnical conditions and landslides possibility especially in the North East of the study area (Baghmisheh town) and shaking at the due time of an earthquake, stopping the construct in the northern parts and extending the settlement construction to the southern parts of the city is inevitable.

Based on the results related to the seismic zonation after implying the soil layer effects on the depth up to the bedrock and amplification, most of the site effect's consequences were observed in the central and center-west part of Tabriz. Such outcomes were due to the existence of the alluvial layers of the current age and the young alluviums and the existence of low resistant and density soil layers. Eventually, these layers' effect on seismic acceleration intensity by amplification reached 15-20% in some points in the provided map.

Declaration of interest

The authors certify that there is no actual or potential conflict of interest in relation of this article.

Author's contributions

Armin Sahebkaram Alamdari: conceptualization, methodology, validation. Rasoul Jani: data curation, writing - original draft preparation. Fariba Behrouz Sarand: investigation, validation. Rouzbeh Dabiri: supervision. Rouzbeh Dabiri: writing - reviewing and editing.

References

Ambraseys, N.N., & Melville, C.P. (1982). *History of Persian earthquakes*. Cambridge: Cambridge University Press.

Amiranlou, H. (2016). *Seismic geotechnical microzonation of Tabriz from the perspective of construction effects based on simulated earthquakes* [PhD thesis]. Islamic Azad University of North Tehran.

Amiranlou, H., Pourkermani, M., Dabiri, R., Qoreshi, M., & Bouzari, S. (2016). The stochastic finite-fault modeling based on a dynamic corner frequency simulating of strong ground motion for earthquake scenario of North Tabriz Fault. *Open Journal of Earthquake Research*, 5(2), 114-121.

Anderson, J., & Hough, S. (1984). A model for the shape of the Fourier amplitude spectrum of acceleration at high frequencies. *Bulletin of the Seismological Society of America*, 74, 1969-1993.

Ansari, A., Noorzad, A., & Zafarani, H. (2009). Clustering analysis of the seismic catalog of Iran. *Computers & Geosciences*, 35(3), 475-486. http://dx.doi.org/10.1016/j.cageo.2008.01.010.

Atesh, E., & Uyanık, O. (2019). Ground and structural interaction using geophysical methods. *Süleyman Demirel University Journal of Natural and Applied Sciences*, 23, 46-60.

Atkinson, G., & Assatourians, K. (2015). Implementation and validation of EXSIM (A Stochastic Finite-Fault Ground-Motion Simulation Algorithm) on the SCEC broadband platform. *Seismological Research Letters*, 86(1), 48-60.

Atkinson, G., Goda, K., & Assatourians, K. (2011). Comparison of nonlinear structural responses for accelerograms simulated from the stochastic finite-fault approach versus the hybrid broadband approach. *Bulletin of the Seismological Society of America*, 101(6), 2967-2980.

Atkinson, G.M., & Silva, W. (1997). An empirical study of earthquake source spectra for California earthquakes. *Bulletin of the Seismological Society of America*, 87, 97-113.

Berberian, M., & Yeats, R.S. (1999). Patterns of historical earthquake rupture in the Iranian Plateau. *Bulletin of the Seismological Society of America*, 89(1), 120-139.

Berberian, M. (1976). *Contribution to the Seismotectonics of Iran (Part II)* (Report, No. 29). Tehran, Iran: Geological Survey of Iran.

Beresnev, I., & Atkinson, G. (1998). FINSIM: a FORTRAN program for simulating stochastic acceleration time histories from finite faults. *Seismological Research Letters*, 69(1), 27-32.

Boore, D.M., & Atkinson, G.M. (2008). Ground-motion-prediction equations for the average horizontal component of PGA, PGV, and 5%-damped PSA at spectral periods between 0.01s and 10 s. *Earthquake Spectra*, 24(1), 99-138.

Boore, D.M. (1983). Stochastic simulation of high-frequency ground motions based on seismological models of the radiated spectra. *Bulletin of the Seismological Society of America*, 73, 1865-1894.

Boore, D.M. (2003). Prediction of ground motion using the stochastic method. *Pure and Applied Geophysics*, 160(3), 635-676.

Boore, D.M. (2005). *SMSIM – FORTRAN programs for simulating ground motions from earthquakes: version 2.3. A revision of OFR 96-80-A: a modified version of*

OFR 00- 509.59. Retrieved in January 20, 2020, from http://daveboore.com/software_online.html

Boore, D.M. (2009). Comparing stochastic point- and finite-source ground-motion simulations: SMSIM and EXSIM. *Bulletin of the Seismological Society of America*, 99(6), 3202-3216.

Boore, D.M., Stewart, J.P., Seyhan, E., & Atkinson, G.M. (2014). NGA-West2 equations for predicting PGA, PGV, and 5% damped PSA for shallow crustal earthquakes. *Earthquake Spectra*, 30(3), 1057-1085.

Bour, M., & Cara, M. (1997). Test of a simple empirical Green's function method on moderate-sized earthquakes. *Bulletin of the Seismological Society of America*, 87, 668-683.

Brune, J.N. (1970). Tectonic stress and the spectra of seismic shear waves from earthquakes. *Journal of Geophysical Research*, 75(26), 4997-5009.

Campbell, K.W., & Bozorgnia, Y. (2008). NGAground motionmodel for the geometric mean horizontal component of PGA, PGV, PGD and 5%-damped linear elastic response spectra for periods ranging from 0.01 to 10 s. *Earthquake Spectra*, 24(1), 139-171.

Drennov, A.F., Dzhurik, V.I., Serebrennikov, S.P., Bryzhak, E.V., & Drennova, N.N. (2013). Acceleration response spectra for the earthquakes of the southwestern flank of the Baikal Rift Zone. *Russian Geology and Geophysics*, 54(2), 223-230.

Eker, A.M., Akgun, H., & Kockar, M.K. (2012). Local site characterization and seismic zonation study by utilizing active and passive surface wave methods: a case study for the northern side of Ankara, Turkey. *Engineering Geology*, 151, 64-81.

Farahani, J. (2015). The cause of dual earthquakes in the East Azarbaijan and the seismicity of the region. In *2nd International Conference on Geotechnical and Urban Seismic Engineering*, City Tabriz. [In persian].

Farahbod, A.M., & Alahyarkhani, M. (2003). Attenuation and propagation characteristics of seismic waves in Iran. In *4th International Conference on Seismology and Earthquake Engineering*, City Tehran.

Groholski, D.R., Hashash, Y.M.A., & Matasovic, N. (2014). Learning of pore pressure response and dynamic soil behavior from downhole array measurements. *Civil and Environmental Engineering*, 61-62, 40-56.

Hamzehloo, H., Alikhanzadeh, A., Rahmani, M., & Ansari, A. (2012). Seismic hazard maps of Iran. In *The 04th World Conference on Earthquake Engineering*, Lisbon.

Hartzell, S. (1978). Earthquake aftershocks as Green's functions. *Geophysical Research Letters*, 5(1), 1-14.

Hashash, Y.M.A., Grohalski, D.R., & Philips, C.A. (2010). Recent advances in non-linear site response analysis. In *5th International Conference on Recent Advances in Geotechnical Earthquake Engineering and Soil Dynamics*, San Diego, California.

Hashash, Y.M.A., Musgrove, M.I., Harmon, J.A., Groholski, D.R., Phillips, C.A., & Park, D. (2016). *DEEPSOIL 6.1: user manual.* Urbana.

Hisada, Y., & Bielak, J. (2003). A theoretical method for computing near fault ground motion in a layered half-spaces considering static offset due a surface faulting, with a physical interpretation of fling step and rupture directivity. *Bulletin of the Seismological Society of America*, 93(3), 1154-1168.

Hoseinpour, N., & Zaré, M. (2009). Seismic hazard assessment of Tabriz, a city in the northwest of Iran. *Journal of the Earth*, 4(2), 21-35.

Irikura, K., & Kamae, K. (1994). Estimation of strong ground motion in broad-frequency band based on a seismic source scaling model and an empirical Green's function technique. *Annali di Geofisica*, 37, 1721-1743.

Irikura, K. (1983). Semi-empirical estimation of strong ground motions during large earthquakes. *Bulletin of the Disaster Prevention Research Institute*, 33, 63-104.

Irikura, K. (1992). The construction of large earthquake by a superposition of small events. *Proceedings of the Tenth World Conference on Earthquake Engineering*, 10, 727-730.

Jackson, J.A., Haines, J., & Holt, W. (1995). The accommodation of Arabia-Eurasia plate convergence in Iran. *Journal of Geophysical Research*, 11, 4114-4109. http://dx.doi.org/10.1029/95JB01294.

Kanamori, H., & Anderson, D.L. (1975). Theoretical basis of some empirical relations in seismology. *Bulletin of the Seismological Society of America*, 65, 1073-1095.

Karimiparidari, S., Zaré, M., & Memarian, H. (2011). New seismotectonic zoning map of Iran. In *6th International Conference on Seismology and Earthquake Engineering*, City Tehran.

Karimzadeh, S., Miyajima, M., Hassanzadeh, R., Amiraslanzadeh, R., & Kamel, B. (2014). A GIS-based seismic hazard, building vulnerability and human loss assessment for the earthquake scenario in Tabriz. *Soil Dynamics and Earthquake Engineering*, 66, 263-280.

Karimzadeh, S., Ozsarac, V., Askan, A., & Erberik, M.A. (2019). Use of simulated ground motions for the evaluation of energy response of simple structural systems. *Soil Dynamics and Earthquake Engineering*, 123, 525-542.

Khoshnevis, N., Taborda, R., Azizzadeh-Roodpish, S., & Cramer, C.H. (2017). Seismic hazard estimation of northern Iran using smoothed seismicity. *Journal of Seismology*, 21(4), 941-964.

Manafi, M. (2012). Seismic potential of Tabriz city and surrounding areas. In *National Symposium on Pathology and Programming of Earthquake Effects*, Tabriz, Iran. [In persian].

Masson, F., Djamour, Y., Van Gorp, S., Chery, J., Tatar, M., Tavakoli, F., Nankali, H., & Vernant, P. (2006). Extension in NW Iran driven by the motion of the South Caspian

Basin. *Earth and Planetary Science Letters*, 252(1-2), 180-188.

Mirzaei, N. (1997). *Seismic Zoning of Iran* [Ph.D. Dissertation]. Institute of Geophysics, State Seismological Bureau.

Mirzaei, N., Gao, M., & Chen, Y.T. (1998). Seismic source regionalization for seismic zoning of Iran: major seismotectonic provinces. *Journal of Earthquake Prediction Research*, 9, 354-394.

Mohammadi, D.S., Firuzi, M., & Asghari Kaljahi, E. (2016). Geological-geotechnical risk in the use of EPB-TBM, case study: tabriz Metro, Iran. *Bulletin of Engineering Geology and the Environment*, 75(4), 1571-1583. http://dx.doi.org/10.1007/s10064-015-0797-7.

Mojarab, M., Memarian, H., Zaré, M., Hossein-Morshedy, A., & Pishahang, M.H. (2013). Modeling of the seismotectonic Provinces of Iran using the self-organizing map algorithm. *Computers & Geosciences*, 59, 41-51.

Motazedian, D., & Atkinson, G. (2005). Stochastic finite-fault model based on dynamic corner frequency. *Bulletin of the Seismological Society of America*, 95(3), 995-1010.

Motazedian, D. (2006). Region-specific key seismic parameters for earthquakes in Northern Iran. *Bulletin of the Seismological Society of America*, 96(4A), 1383-1395.

Nogol-Sadat, M.A.A. (1994). *Seismotectonic map of Iran, Teritise on the Geology of Iran. 0001110111 Scale Tehran, Iran.* Iran.

Nowroozi, A.A. (1996). Seismotectonic provinces of Iran. *Bulletin of the Seismological Society of America*, 55, 139-195.

Park, D., & Hashash, Y.M.A. (2005). Evaluation of seismic site factors in the Mississippi Embayment. II. Probabilistic seismic hazard analysis with nonlinear site effects. *Soil Dynamics and Earthquake Engineering*, 25(2), 145-156. http://dx.doi.org/10.1016/j.soildyn.2004.10.003.

Pitilakis, K., Gazepis, C., & Anastasiadis, A. (2004). Design response spectra and soil classification for seismic code provisions. In *Proceedings of 13th World Conference on Earthquake Engineering* (Paper No. 2904). Vancouver, Canada.

Mohammad Raza, P. M., Hanyeh, Y. S., & H. Dalir Karim, H. (2018). Evaluation of resilience of vital uses of Tabriz metropolis against natural earthquake risk. *Geographical Research in Urban Planning*, 6(1), 55-74. [In persian].

Rodríguez-Marek, A., Bray, J.D., & Abrahamson, N.A. (2001). An empirical geotechnical seismic site response procedure. *Earthquake Spectra*, 17(1), 65-87.

Rustaei, S., & Sari Sarraf, B. (2006). Zoning of environmental hazards affecting the physical development of Tabriz. *Journal of Land*, 10, 126-110. [In persian].

Samaei, M., Miyajima, M., & Yazdani, A. (2014). Prediction of strong ground motion using stochastic finite fault method: a case study of Niavaran Fault, Tehran. *Geodynamics Research International Bulletin*, 2(4), 13-23.

Scandella, L., Lai, C.G., Spallarossa, D., & Corigliano, M. (2011). Ground shaking scenarios at the town of Vicoforte, Italy. *Soil Dynamics and Earthquake Engineering*, 31(5-6), 757-772.

Schneider, J.F., Silva, W.J., & Stark, C. (1993). Ground motion model for the 1989 M 6.9 Loma Prieta earthquake including effects of source, path, and site. *Earthquake Spectra*, 9(2), 251-287.

Shoja-Taheri, J. (1984). Acceleration of the 1978 Tabas (Iran) Earthquake: The Generalized Records of Correlation between the Strong Motion Parameters in Different Frequency Bands. In *Regional Assembly of IASPEI*, Heyderabad, India [Oral presentation].

Shoja-Taheri, J., Naserieh, S., & Hadi, G. (2010). A test of the applicability of NGA models to the strong ground-motion data in the Iranian plateau. *Journal of Earthquake Engineering*, 14(2), 278-292.

Shreyasvi, C., Venkataramana, K., & Chopra, S. (2019). Local site effect incorporation in probabilistic seismic hazard analysis: a case study from southern peninsular India, an intraplate region. *Soil Dynamics and Earthquake Engineering*, 123, 381-398.

Siahkali Moradi, A., Hatsfeld, D., & Pal, A. (2008). Research crust velocity structure and mechanism faulting in Tabriz Strike Slip Region. *Journal of Geology Science*, (70).

Sinaiean, F. (2006). *A study of the strong ground motions in Iran* [Ph.D. thesis]. International Institute of Earthquake Engineering and Seismology.

Sinaiean, F., Zaré, M., & Fukushima, Y. (2007). A study on the empirical PGA attenuation relationships in Iran. In *Proceedings of the 5th International Conference on Seismology and Earthquake Engineering*, Tehran.

Tavakoli, B. (1996). *Major seismotectonic Provinces of Iran*. Tehran, Iran: International Institute of Earthquake Engineering and Seismology (IIEES). [In Persian].

Uyanık, O. (2015). Predetermination of earthquake heavy damage areas and importance of macro and micro zoning for urban planning. *Süleyman Demirel University Journal of Natural and Applied Sciences*, 19(2), 24-38.

Uyanık, O., Ekinci, B., & Uyanık, N.A. (2013). Liquefaction analysis from seismic velocities and determination of lagoon limits Kumluca/Antalya example. *Journal of Applied Geophysics*, 95, 90-103.

Uyanık, O., Türker, E., & İsmailov, T. (2006). Sığ Sismik Mikro-Bölgeleme ve Burdur/Türkiye Örneği. *Ekologiya ve Su Teserrüfatı, Elmi-Texniki ve istehsalat Jurnalı*, 1, 9-15.

Verdugo, R., Ochoa-Cornejo, F., Gonzalez, J., & Valladares, G. (2019). Site effect and site classification in areas with large earthquakes. *Soil Dynamics and Earthquake Engineering*, 126, 105071. http://dx.doi.org/10.1016/j.soildyn.2018.02.002.

Wang, Z., Su, J., Liu, C., & Cai, X. (2015). New insights into the generation of the 2013 Lushan Earthquake (M_s 7.0), China. *Journal of Geophysical Research. Solid Earth*, 120(5), 3507-3526.

Wells, D.L., & Coppersmith, K.J. (1994). New empirical relationships among magnitude, rupture length, rupture

width, rupture area, and surface displacement. *Bulletin of the Seismological Society of America*, 84(4), 974-1002.

Yaghmaei-Sabegh, S., & Hassani, B. (2020). Investigation of the relation between Vs30 and site characteristics of Iran based on horizontal-to-vertical spectral ratios. *Soil Dynamics and Earthquake Engineering*, 128, 105899.

Yaghmaei-Sabegh, S., & Motallebzade, R. (2012). An effective procedure for seismic hazard analysis including nonlinear soil response. *Natural Hazards*, 64(2), 1731-1752.

Yazdani, A., & Kowsari, M. (2013). Earthquake ground-motion prediction equations for northern Iran. *Natural Hazards*, 69(3), 1877-1894.

Zaré, M., & Memarian, H. (2000). *Simulation of earthquakes intensity in Iran, research report of Iranian Red Crescent*. Tehran, Iran. 41 p. [In Persian].

Zaré, M. (2000). Investigation of tectonic seismology and slope vector analysis in Lake District of Urmia. In *International Institute of Seismology and Earthquake Engineering*, Tehran. [In Persian].

Zaré, M. (2001). The risk of earthquakes and construction in the north of Tabriz fault zone and fault zone of earthquake faults in Iran. In *International Institute of Seismology and Earthquake Engineering*, Tehran. [In Persian].

Zaré, M., Bard, P.Y., & Ghafory-Ashtiany, M. (1999). Site characterizations for the Iranian strong motion network. *Soil Dynamics and Earthquake Engineering*, 18(2), 101-123.

Zaré, M., Karimi-Paridari, S., & MonaLisa, (2009). An investigation on Balakot, Muzaffarabad (Pakistan) earthquake, 8 Oct. 2005, Mw 7.6; geological aspects and intensity distribution. *Journal of Seismology*, 13(3), 327-337.

Zonno, G., Basili, R., Meroni, F., Musacchio, G., Mai, P.M., Valensise, G., & Boschi, E. (2012). High-frequency maximum observable shaking map of Italy from fault sources. *Bulletin of Earthquake Engineering*, 10(4), 1075-1107.